NANO LETTERS

LETTER

pubs.acs.org/NanoLett

Enhanced Thermoelectric Figure of Merit of p-Type Half-Heuslers

Xiao Yan,[†] Giri Joshi,[†] Weishu Liu,[†] Yucheng Lan,[†] Hui Wang,[†] Sangyeop Lee,[‡] J. W. Simonson,[§] S. J. Poon,[§] T. M. Tritt,[∥] Gang Chen,*[,‡] and Z. F. Ren*[,†]

[†]Department of Physics, Boston College, Chestnut Hill, Massachusetts 02467, United States

[‡]Department of Mechanical Engineering, Massachusetts Institute of Technology, Cambridge, Massachusetts 02139, United States

[§]Department of Physics, University of Virginia, Charlottesville, Virginia 22904-4714, United States

[∥]Department of Physics & Astronomy, Clemson University, Clemson, South Carolina 29634, United States

ABSTRACT: Half-Heuslers would be important thermoelectric materials due to their high temperature stability and abundance if their dimensionless thermoelectric figure of merit (ZT) could be made high enough. The highest peak ZT of a p-type half-Heusler has been so far reported about 0.5 due to the high thermal conductivity. Through a nanocomposite approach using ball milling and hot pressing, we have achieved a peak ZT of 0.8 at 700 °C, which is about 60% higher than the best reported 0.5 and might be good enough for consideration for waste heat recovery in car exhaust systems. The improvement comes from a simultaneous increase in Seebeck coefficient and a significant decrease in thermal conductivity due to nanostructures. The samples were made by first forming alloyed ingots using arc melting and then creating nanopowders by ball milling the ingots and finally obtaining dense bulk by hot pressing. Further improvement in ZT is expected when average grain sizes are made smaller than 100 nm.

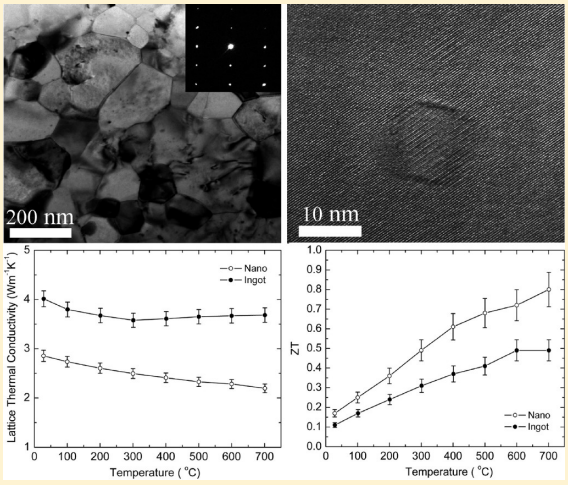

KEYWORDS: Thermoelectrics, half-Heusler, nanocomposite, ball milling, hot pressing

The potential of half-Heusler alloys for high temperature thermoelectric power generation has been discussed.[1,2] Half-Heuslers have the cubic MgAgAs type of structure, forming three interpenetrating face-centered-cubic (fcc) sublattices and one vacant sublattice.[3] Until recently the reported p-type half-Heusler alloys are mostly based on the formula MCoSb, where M is Ti, Zr, or Hf.[4−7] The high substitutability of the three lattice sites (M, Co, and Sb) provides many opportunities for tuning the electronic and lattice properties of the half-Heuslers. Through partial elemental substitution, the large lattice thermal conductivity of half-Heusler compounds is expected to be greatly reduced due to mass fluctuation and strain field effects.[4−7] However, the thermal conductivity of p-type half-Heusler alloys reported so far still remains very high (higher than 4 W m^{-1} K^{-1}),[4−7] which prevents ZT from reaching a meaningful value. The highest ZT of about 0.5 in p-type $Zr_{0.5}Hf_{0.5}CoSb_{0.8}Sn_{0.2}$ was achieved at 1000 K with a thermal conductivity of 4.1 W m^{-1} K^{-1} at 300 K and 3.6 W m^{-1} K^{-1} at 1000 K.[8] Such a thermal conductivity is still very high due to mainly the contribution of lattice thermal conductivity. Besides alloy scattering via partial elemental substitution, boundary scattering can be introduced to further reduce the thermal conductivity.[9] Even though ball milling was attempted to reduce the thermal conductivity due to the decreased average grain size, the ZT improvement was minimal due to the still too large average grain size of at least 1 μm.[10−12] On the basis of our success on achieving grain sizes much smaller than 1 μm in a number of materials by ball milling and hot pressing,[13−18] we have succeeded in achieving grain sizes smaller than 200 nm in p-type half-Heusler samples with a composition of $Zr_{0.5}Hf_{0.5}CoSb_{0.8}Sn_{0.2}$ by ball milling the alloyed ingot into nanopowders and then hot pressing them into dense bulk samples, resulting in a simultaneous increase in Seebeck coefficient and a significant decrease in thermal conductivity, which led to a 60% improvement in peak ZT from 0.5 to 0.8 at 700 °C.

Experimental Procedure. In a typical experiment, an alloyed ingot with a composition of $Zr_{0.5}Hf_{0.5}CoSb_{0.8}Sn_{0.2}$ was loaded into a jar with grinding balls and then subjected to a mechanical ball-milling process. For different ball-milling time intervals, a small amount of as-milled powder was taken out for size investigation by transmission electron microscopy (TEM) (JEOL 2010). Correspondingly, some nanopowders were pressed into pellets with a diameter of 12.7 mm by the direct current induced hot-press method. The freshly fractured surfaces of the as-pressed

Received: October 3, 2010
Revised: December 12, 2010
Published: December 22, 2010

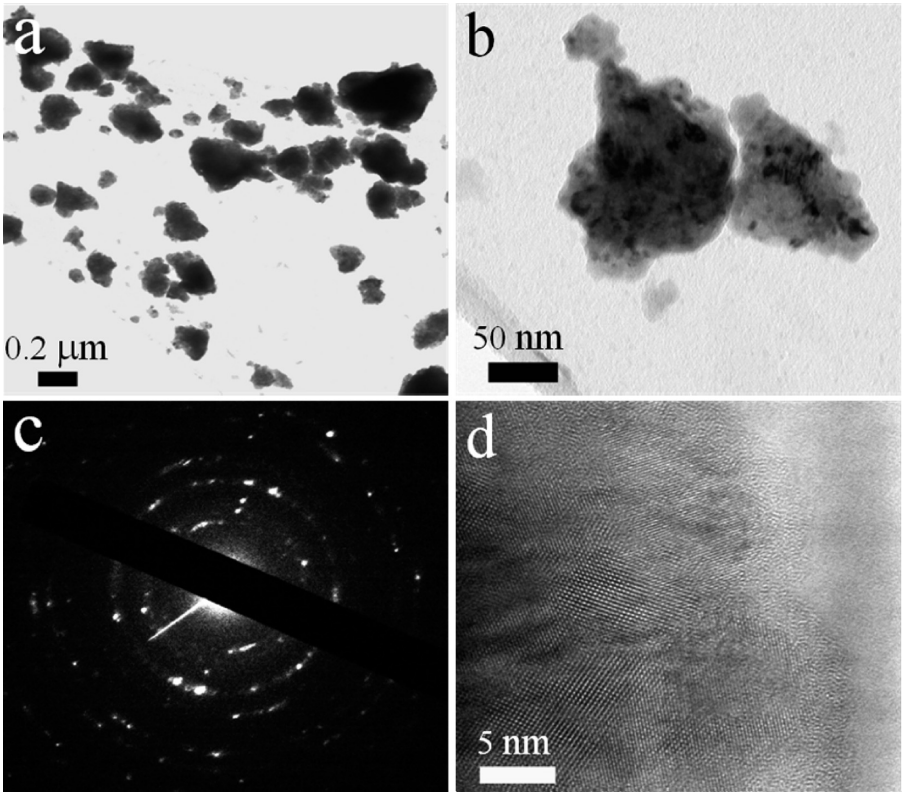

Figure 1. (a) Low and (b) medium magnification TEM images. (c) Selected area electron diffraction patterns. (d) High magnification TEM image of the ball-milled nanopowders. The selected area electron diffraction patterns in (c) show the multicrystalline nature of an agglomerated cluster in (b).

samples were observed by scanning electron microscopy (SEM) (JEOL 6340F) and TEM to show the grain size of the samples.

To study the thermoelectric properties, polished bars of about $2 \times 2 \times 12$ mm and disks of 12.7 mm in diameter and 2 mm in thickness were made. The bar samples were used to measure the electrical conductivity and Seebeck coefficient, and the disk samples were used to measure the thermal conductivity. The four-probe electrical conductivity and the Seebeck coefficient were measured using commercial equipment (ULVAC, ZEM3). The thermal diffusivity was measured using a laser flash system (LFA 457 Nanoflash, Netzsch Instruments, Inc.). Specific heat was determined by a DSC instrument (200-F3, Netzsch Instruments, Inc.). The volume density was measured by the Archimedes method. The thermal conductivity was calculated as the product of thermal diffusivity, specific heat, and volume density. The uncertainties are 3% for electrical conductivity, thermal diffusivity and specific heat, and 5% for the Seebeck coefficient, leading to an 11% uncertainty in ZT.

We have repeated the experiments more than 10 times and have confirmed that the peak ZT values were reproducible within 5%.

Results and Discussions. Figure 1 shows the TEM images of the ball-milled nanopowders. The low (Figure 1a) and medium (Figure 1b) magnification TEM images show that the average cluster size of the nanopowders ranges from 20 to 500 nm. However, those big clusters are actually agglomerates of many much smaller crystalline grains, which are confirmed by the corresponding selected area electron diffraction (SAED) patterns (Figure 1c) obtained inside a single cluster (Figure 1b). The high-resolution TEM image (Figure 1d) shows that the sizes of the small grains are in the range of 5−10 nm.

Figure 2 displays the TEM images of the as-pressed bulk samples pressed from the ball-milled powder. A low magnification TEM image is presented in Figure 2a, from which we can see that the grain sizes are in the range of 50−300 nm with an estimated average size being about 100−200 nm. Therefore, there is a significant grain growth during the hot-pressing process. The SAED pattern (inset of Figure 2a) of each individual grains indicates that the individual grains are single crystalline. The high-resolution TEM image (Figure 2b) demonstrates the good crystallinity inside each individual grain. Figure 2c shows one nanodot embedded inside the matrix, such dots are commonly observed in most of the grains. The compositions of both the nanodot and its surrounding areas are checked by energy dispersive spectroscopy (EDS), showing Hf rich and Co deficient for the nanodot. Another feature pertaining to our sample is that small grains (~30 nm) are also common (Figure 2d), which have similar composition to the surrounding bigger grains as determined by EDS. We suspect that the nonuniformity in both the grain sizes and the composition contributes to the reduction of thermal conductivity.

The temperature-dependent thermoelectric (TE) properties of the hot-pressed $Zr_{0.5}Hf_{0.5}CoSb_{0.8}Sb_{0.2}$ bulk samples in comparison with that of the ingot are plotted in Figure 3. For all of the samples examined, the temperature dependence of the electrical conductivity was found to exhibit semimetallic or degenerate semiconductor behavior (Figure 3a). Specifically, the electrical conductivities of all the ball-milled and hot-pressed samples are lower than that of the ingot. We have measured the mobility and carrier concentration at room temperature to be 3.86 $cm^2\ V^{-1}\ s^{-1}$ and $1.6 \times 10^{21}\ cm^{-3}$, respectively. The mobility is lower than the previously reported value while the carrier concentration is higher.[8]

dx.doi.org/10.1021/nl104138t |*Nano Lett.* 2011, 11, 556–560

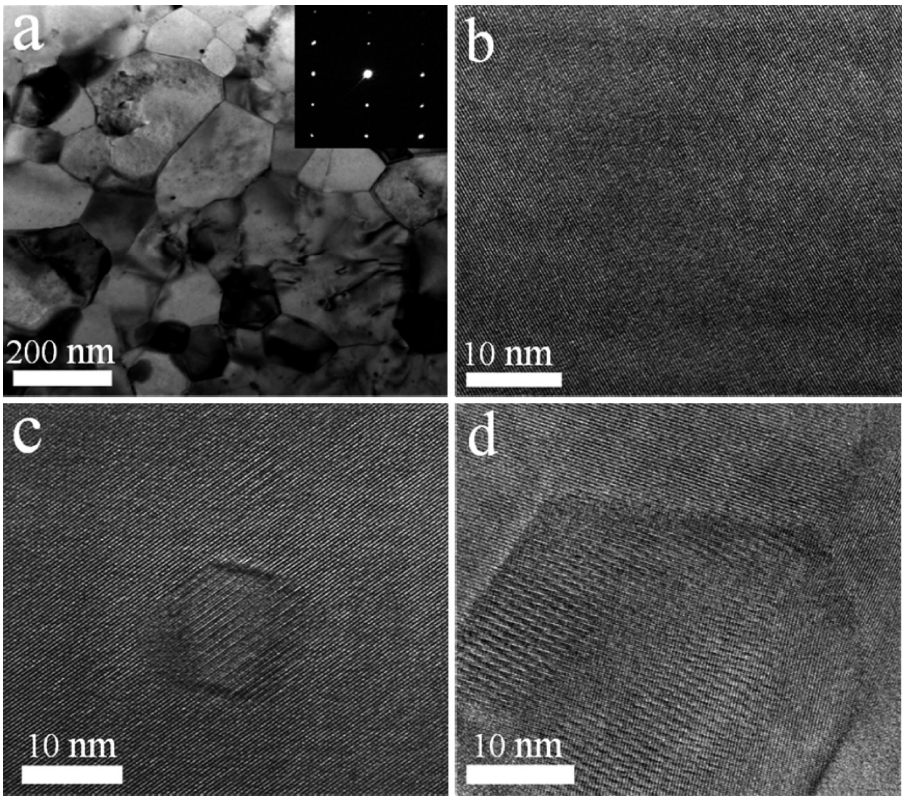

Figure 2. TEM images of hot-pressed nanostructured samples under low (a) and high magnifications (b−d). The inset in (a) is the selected area electron diffraction patterns showing the single crystalline nature of the individual grains.

Electrical conductivities of our ball-milled samples decrease slowly at the higher temperature range. The Seebeck coefficients (Figure 3b) of our ball-milled samples are higher than that of the ingot for the whole temperature range. These facts strongly indicate that grain boundaries may be trapping electrons, leading to increased holes in the sample and energy filtering effect[19] where low energy holes are preferentially scattered at the grain boundaries. As a result of the improvement in the Seebeck coefficient and a slight decrease in the electrical conductivity, the power factor (Figure 3c) of our ball-milled and hot-pressed samples are higher than that of the ingot. The total thermal conductivity of our ball-milled and hot-pressed samples (Figure 3d) decreases gradually with temperature up to 500 °C and does not change too much after that, which shows a much weaker bipolar effect, consistent with our earlier report in other thermoelectric materials with nanostructures.[13] The reduction of the thermal conductivity in our ball-milled and hot-pressed nanostructured samples compared with the ingot is mainly due to the increased phonon scattering at the numerous interfaces of the random nanostructures. To get a quantitative view of the effect of ball milling and hot pressing on phonon transport, the lattice thermal conductivity (κ_l) was estimated by subtracting the electronic contribution (κ_e) from the total thermal conductivity (κ). The electronic contribution to the thermal conductivity (κ_e) can be estimated using the Wiedemann−Franz law. The Lorenz number can be obtained from the reduced Fermi energy, which can be calculated from the Seebeck coefficient at room temperature and the two band theory.[20] Within expectation, the lattice part of the thermal conductivity (Figure 3e) decreases with temperature. For the ingot sample, we obtained κ_e = 0.7 W m^{1-} K^{-1} and κ_l = 4.01 W m^{1-} K^{-1} at room temperature, whereas for the ball-milled and hot-pressed samples κ_e = 0.54 W m^{1-} K^{-1} due to a lower electrical conductivity and κ_l = 2.86 W m^{1-} K^{-1} at room temperature. The lattice thermal conductivity of the ball-milled and hot-pressed samples at room temperature is about 29% lower than that of the ingot, which is mainly due to a stronger boundary scattering in the nanostructured sample. It appears that the lattice part is still a large portion of the total thermal conductivity. If the average grain size below 100 nm is achieved during hot pressing, the thermal conductivity can be expected to be further reduced. The slightly improved power factor, coupled with the significantly reduced thermal conductivity, makes the ZT (Figure 3f) of our ball-milled and hot-pressed samples greatly improved in comparison with that of the ingot. The peak ZT of all our ball-milled and hot-pressed samples reached 0.8 at 700 °C, a 60% improvement over the highest reported ZT value of 0.5 obtained in the ingot,[8] showing great promise as p-type material for high temperature applications.

We also show the specific heat (Figure 4a) and thermal diffusivity (Figure 4b) of our ball-milled and hot-pressed samples in comparison with that of the ingot sample. The specific heat (Figure 4a) of both the ingot and the ball-milled and hot-pressed samples increases steadily with temperature up to 600 °C (the limit of our DSC measurement instrument). The specific heat value at 700 °C was obtained by a reasonable extrapolation. The specific heat difference of about 3% is within the experimental error of the measurement. It is very clear that the major decrease is in thermal diffusivity (Figure 4b) with our ball-milled and hot-pressed sample consistently lower than that of the ingot sample for the whole temperature range, which is the solid evidence showing the effect of grain boundaries on phonon scattering.

dx.doi.org/10.1021/nl104138t |*Nano Lett.* 2011, 11, 556–560

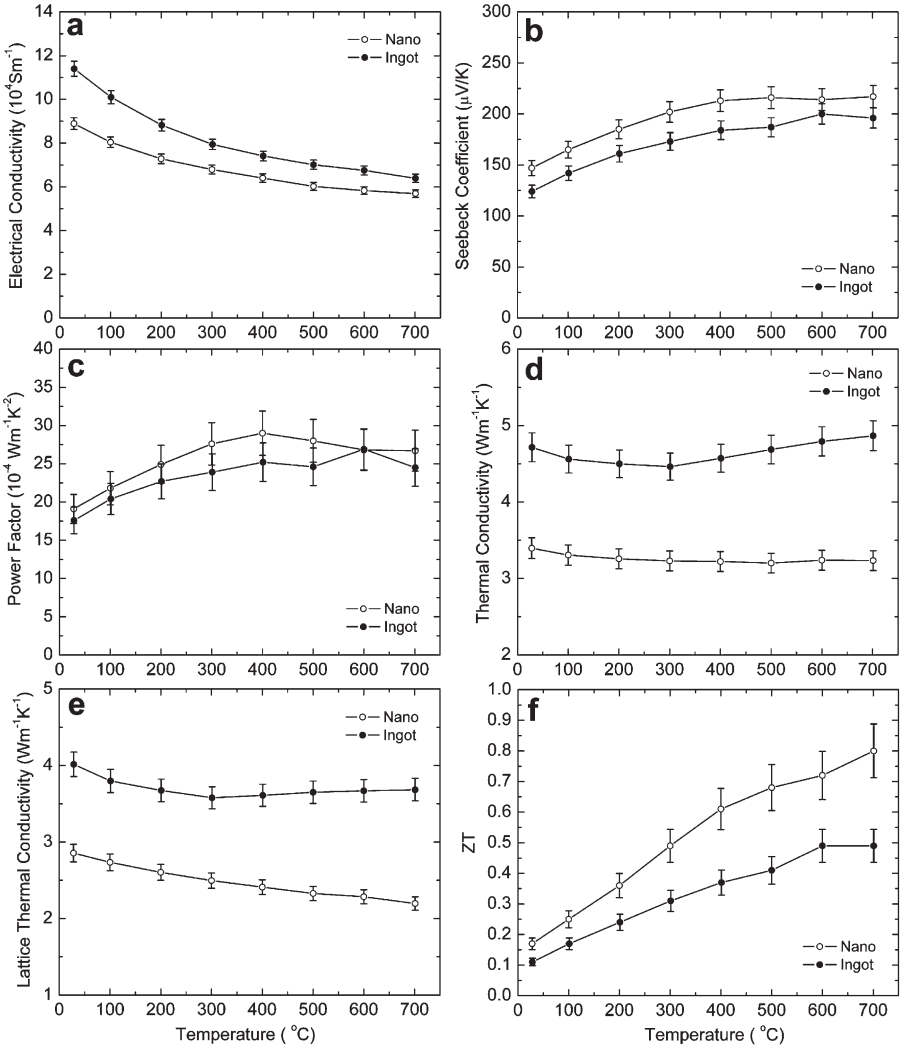

Figure 3. Temperature-dependent (a) electrical conductivity, (b) Seebeck coefficient, (c) power factor, (d) total thermal conductivity, (e) lattice part of thermal conductivity, and (f) ZT of ball-milled and hot-pressed sample in comparison with that of the ingot.

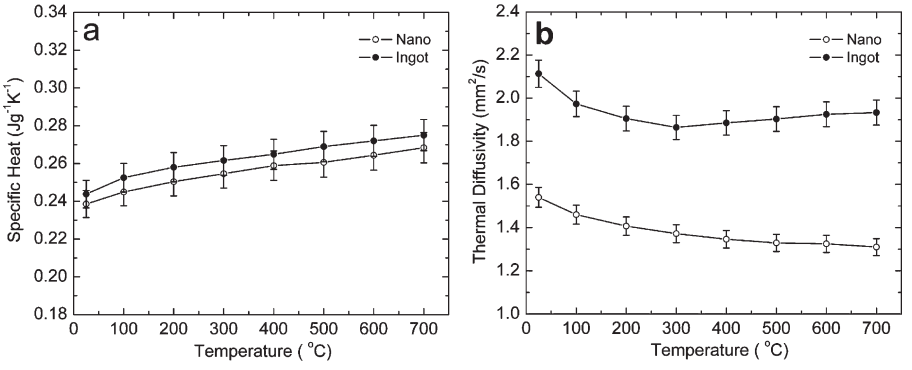

Figure 4. Temperature-dependent specific heat (a) and thermal diffusivity (b) of ball-milled and hot-pressed sample in comparison with that of the ingot.

By comparison with the data on ingot samples previously reported,[8] we found that the resistivity of our ingot sample is almost the same as the reported value, and the Seebeck coefficient is higher, which leads to a higher power factor. However, the thermal conductivity of our ingot sample is proportionally higher than the reported value,[8] which leads to the same ZT of our ingot samples as the reported value.[8] These small differences in individual properties may be due to some minor differences on sample preparation procedures, which is very reasonable and understandable.

Since the ingot samples are made and measured by the same person on the same machine with the nanostrcutured samples,

dx.doi.org/10.1021/nl104138t |*Nano Lett.* 2011, 11, 556–560

we are confident that the enhancement of ZT in the nanostructured samples made by ball milling and hot pressing in this study is real and significant.

Although we have achieved a significant enhancement in ZT of p-type half-Heusler alloys, there remains much room for further improvement. The average grain size of 100−200 nm of our hot pressed bulk samples is much larger than the 5−10 nm of the ball-milled precursor nanopowders, which is why the lattice thermal conductivity is still very high. If we can preserve the grain size of the original nanopowders, a much lower thermal conductivity and thus a much higher ZT can be expected. Besides boundary scattering, minor dopants may also be introduced to enhance the alloy scattering, provided that they do not deteriorate the electronic properties. The ZT values we report here are very reproducible within 5% from run to run on more than 10 samples made under the similar conditions.

Conclusions. By employing the nanocomposite approach using ball milling and hot pressing, we have achieved a slightly higher Seebeck coefficient and a significantly lower thermal conductivity in p-type half-Heusler materials in comparison with the ingot, both of which are associated with the embedded nanostructures and small grain size. A significant improvement in peak ZT was observed in the ball-milled and hot-pressed samples with the peak ZT reaching 0.8 at 700 °C, which is 60% higher than that of the highest reported value in an ingot. Preserving the size of the original nanopowders remains an issue.

AUTHOR INFORMATION

Corresponding Author
*E-mail: gchen2@mit.edu and renzh@bc.edu.

ACKNOWLEDGMENT

The work is funded by the US Department of Energy under Contract Number DOE DE-FG02-00ER45805 (Z.F.R.) and the "Solid State Solar-Thermal Energy Conversion Center (S^3TEC)", an Energy Frontier Research Center funded by the U.S. Department of Energy, Office of Science, Office of Basic Energy Sciences under Award Number: DE-SC0001299 (G.C. and Z.F.R.).

REFERENCES

(1) Uher, C.; Yang, J.; Hu, S.; Morelli, D. T.; Meisner, G. P. *Phys. Rev. B* **1999,** *59,* 8615.
(2) Poon, S. J. *Recent Trends in Thermoelectric Materials Research II, Semiconductors and Semimetals*; Tritt, T. M., Ed.; Academic: New York, 2001; Vol. 70, p 37.
(3) Jeischko, W. *Metall. Trans.* **1970,** *1,* 3159.
(4) Xia, Y.; Bhattacharya, S.; Ponnambalam, V.; Pope, A. L.; Poon, S. J.; Tritt, T. M. *J. Appl. Phys.* **2000,** *88,* 1952.
(5) Sekimoto, T.; Kurosaki, K.; Muta, H.; Yamanaka, S. *J. Alloys Compd.* **2006,** *407,* 326.
(6) Wu, T.; Jiang, W.; Li, X. Y.; Zhou, Y. F.; Chen, L. D. *J. Appl. Phys.* **2007,** *102,* No. 103705.
(7) Ponnambalam, V.; Alboni, P. N.; Edwards, J.; Tritt, T. M.; Culp, S. R.; Poon, S. J. *J. Appl. Phys.* **2008,** *103,* No. 063716.
(8) Culp, S. R.; Simonson, J. W.; Poon, S. J.; Ponnambalam, V.; Edwards, J.; Tritt, T. M. *Appl. Phys. Lett.* **2008,** *93,* No. 022105.
(9) Sharp, J. W.; Poon, S. J.; Goldsmid, H. J. *Phys. Status Solidi* **2001,** *187,* 507.
(10) Tritt, T. M.; Bhattacharya, S.; Xia, Y.; Ponnambalam, V.; Poon, S. J.; Thadhani, N. *ICT'01* **2001,** 7.
(11) Katsuyama, S.; Kobayashi, T. *Mater. Sci. Eng., B* **2010,** *166,* 99.
(12) Xie, W. J.; Tang, X. F.; Zhang, Q. J. *Chin. Phys. (Beijing, China)* **2007,** *16,* 3549.
(13) Poudel, B.; Hao, Q.; Ma, Y.; Lan, Y. C.; Minnich, A.; Yu, B.; Yan, X.; Wang, D. Z.; Muto, A.; Vashaee, D.; Chen, X. Y.; Liu, J. M.; Dresselhaus, M. S.; Chen, G.; Ren, Z. F. *Science* **2008,** *320,* 634.
(14) Ma, Y.; Hao, Q.; Poudel, B.; Lan, Y. C.; Yu, B.; Wang, D. Z.; Chen, G.; Ren, Z. F. *Nano Lett.* **2008,** *8,* 2580.
(15) Joshi, G.; Lee, H.; Lan, Y. C.; Wang, X. W.; Zhu, G. H.; Wang, D. Z.; Gould, R. W.; Cuff, D. C.; Tang, M. Y.; Dresselhaus, M. S.; Chen, G.; Ren, Z. F. *Nano Lett.* **2008,** *8,* 4670.
(16) Wang, X. W.; Lee, H.; Lan, Y. C.; Zhu, G. H.; Joshi, G.; Wang, D. Z.; Yang, J.; Muto, A. J.; Tang, M. Y.; Klatsky, J.; Song, S.; Dresselhaus, M. S.; Chen, G.; Ren, Z. F. *Appl. Phys. Lett.* **2008,** *93,* No. 193121-1.
(17) Zhu, G. H.; Lee, H.; Lan, Y. C.; Wang, X. W.; Joshi, G.; Wang, D. Z.; Yang, J.; Vashaee, D.; Guilbert, H.; Pillitteri, A.; Dresselhaus, M. S.; Chen, G.; Ren, Z. F. *Phys. Rev. Lett.* **2009,** *102,* No. 196803-1.
(18) Yang, J.; Hao, Q.; Wang, H.; Lan, Y. C.; He, Q. Y.; Minnich, A.; Wang, D. Z.; Harriman, J. A.; Varki, V. M.; Dresselhaus, M. S.; Chen, G.; Ren, Z. F. *Phys. Rev. B* **2009,** *80,* No. 115329.
(19) Heremans, J. P.; Thrush, C. M.; Morelli, D. T. *Phys. Rev. B* **2004,** *70,* No. 115334.
(20) Liu, W. S.; Zhang, B. −P.; Li, J. −P.; Zhang, H. −L.; Zhao, L. −D. *J. Appl. Phys.* **2007,** *102,* No. 103717.